

An Analysis of Nonstationary Noise in LIGO Detectors

Andrew Cupps

May 12, 2024

Abstract

Gravitational waves are physical phenomena predicted by the theory of general relativity. Gravitational wave detectors such as those constituting the Laser Interferometry Gravitational-Wave Observatory are used by researchers to identify and analyze gravitational waves. The match filtering algorithms used to identify and classify gravitational wave signals assume stationary noise; in this paper, I investigate this assumption and find three examples of nonstationary noise in LIGO detectors, including nonstationary noise signals near 304 Hz and 512 Hz, as well as strongly-correlated and oscillating noise levels between low frequencies.

1 Introduction & Background

1.1 Gravitational Waves & Detectors

General relativity is a theory explaining gravity not as a force between masses (as it is defined in traditional Newtonian mechanics) but instead as the result of warpage in spacetime resulting from the concentration of mass [1]. As shown in derivations by Einstein and Rosen, general relativity theory mathematically implies the existence of gravitational waves which propagate outward from the changing distribution of mass [2]. The orbits and mergers of binary systems of massive and compact celestial bodies – specifically neutron stars and black holes – can generate gravitational waves large enough to be detected on Earth; by observing gravitational waves, researchers can gain insights into processes affecting these objects and other processes that would otherwise be unobservable using electromagnetic waves [3].

Gravitational wave detectors utilize a technique called interferometry to directly measure the effects of gravitational waves. A Michelson interferometer (see Figure 1), the style used in gravitational wave detectors, consists of two orthogonal arms; as a wave passes through a detector, it causes the length of one arm to increase while the other decreases in an oscillating fashion. A laser beam is used to measure any offset in the length of one arm relative to the other; this is then used to calculate the proportional displacement caused by a wave, called the strain.

Oscillations in strain are used to identify gravitational wave signals, but signal noise (see Section 1.2) can interfere with a detector's ability to do so; sources of noise in detectors include quantum noise, test mass thermal noise, suspension thermal noise, fluctuating gravitational forces due to seismic waves, residual gas noise, and more [4]. This noise is especially problematic because the effects of actual gravitational wave signals are minuscule; as an example, the first successfully observed gravitational wave signal had a peak strain of only about 10^{-21} , or a displacement amplitude of 4×10^{-18} meters [5].

There are two of these gravitational wave detectors operating in the United States: one in Hanford, Washington, and one in Livingston, Louisiana. These two detectors together compose the Laser Interferometry Gravitational-Wave Observatory (LIGO), which operates in collaboration with other detectors around the world such as the Virgo observatory. In this paper, I will be analyzing the nature of the noise observed in LIGO detectors.

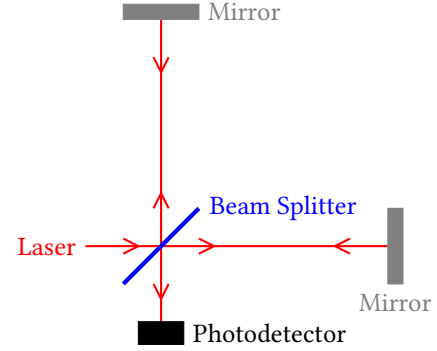


Figure 1. Simplified diagram of a Michelson interferometer, the style of interferometer used in LIGO detectors.

1.2 Signal Processing & Noise

In gravitational wave detectors, noise refers to measured strain that is not the result of a gravitational wave. As mentioned in 1.1, noise may originate from any of a number of different sources, and can mask actual gravitational wave signals, thereby making it more difficult to detect waves. For this reason, a variety of both physical and algorithmic techniques are used to limit the amount of noise detected [4]. Here, I focus on the algorithmic techniques.

LIGO detectors use matched filtering to extract gravitational wave signals from noisy data. In this process, a template (a waveform of what the signal is expected to look like) and noisy data are mathematically combined to produce a matched filter output, which is then used to generate a time-dependent signal-to-noise ratio (SNR); if there is a signal in the data, then it will be present at time t where the SNR is maximized.

As defined by Allen, et al. [6], the matched filter output $z(t)$ is expressed as follows:

$$z(t) = 4 \int_0^\infty \frac{\tilde{h}(f)\tilde{s}(f)}{S_n(f)} e^{2\pi i f t} df \quad (1)$$

where $\tilde{h}(f)$ is the Fourier transform as a function of frequency of the template $h(t)$; $\tilde{s}(f)$ is the Fourier transform as a function of frequency of the detector data $s(t)$; and $S_n(f)$ is the power spectral density (see 1.2.1) of the noise.

A signal to noise ratio (SNR) can then be obtained via the equation:

$$\rho(t) = \frac{|z(t)|}{\sigma} \quad (2)$$

where σ can be found using the equality:

$$\sigma^2 = 4 \int_0^\infty \frac{|\tilde{h}(f)|^2}{S_n(f)} df \quad (3)$$

in which $\tilde{h}(f)$ and $S_n(f)$ are the same as defined in Equation 1. By setting $h(t)$ to be an expected gravitational wave signal generated by numerical simulations, and using a time series of detector data for $s(t)$, as well as its baseline noise level to generate $S_n(f)$, optimal matched filtering can be used to evaluate the presence of a signal similar to $h(t)$ within the detector data $s(t)$.

1.2.1 Power Spectral Density The function $s(t)$ representing the strain measured by a gravitational wave detector over a certain time period can be approximated using a sum of many waves with different frequencies. The power spectral density (PSD) of the strain estimates the contribution of each individual frequency over a range of frequencies to $s(t)$.

Consider white noise, which is random but has a Gaussian distribution about a mean μ with a standard deviation σ . Since the noise is random, the PSD should be similar across all relevant frequencies (as can be seen in Figure 2), since there is no pattern or periodicity to the noise.

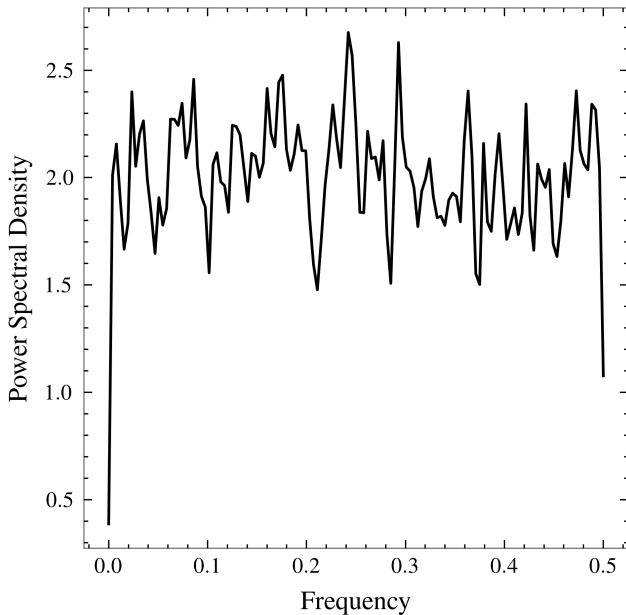


Figure 2. Power spectral density plot of randomly-generated white noise.

However, a PSD generated from the data of a gravitational wave detector will not be relatively flat like that seen in Figure 2. Instead, as seen in Figure 3, the nature of the noise sources results in visible trends in the PSD as well as spikes at certain frequency values [4]. For instance, Figure 3 shows higher PSD values at low frequencies, indicating that low frequency noise has a higher contribution to the overall noise in the detector than higher frequencies, with the exception of spikes in PSD at certain frequencies.

PSDs are an essential part of this paper; in addition to being an important part of the matched filtering algorithm (where $S_n(f)$ is the PSD of noise in the detector), they are useful for analyzing the periodicity of the noise itself.

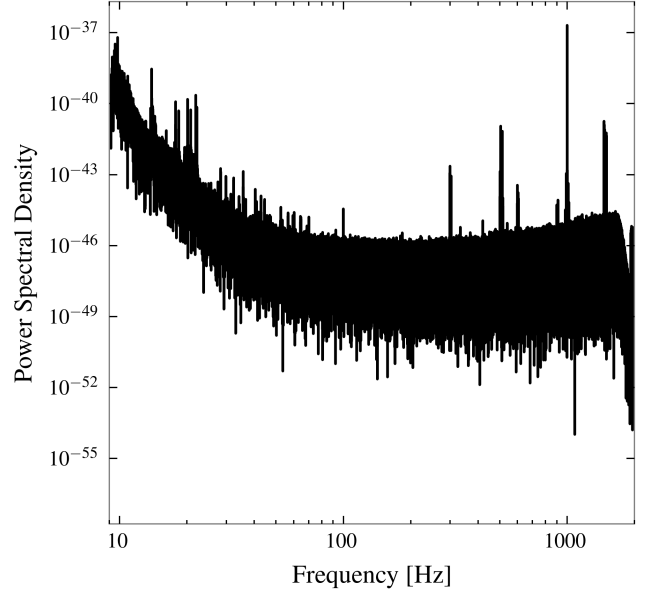


Figure 3. Power spectral density plot of a sample of noise data from the LIGO Hanford detector, plotted on dual logarithmic-scale axes.

1.2.2 Stationarity An important characteristic of noise is stationarity. Noise may be described as stationary or nonstationary depending on whether its behavior is constant over time. Describing noise as stationary does not mean that the measured noise level is constant over time; instead, the actual noise level is expected to vary, but the underlying statistical properties (for example, the distribution of values, or the power spectral density) are constant [7]. For instance, the actual measured value of a stationary white noise signal is random at any given time, but the power spectral density would look similar to that seen in Figure 2 and remain the same regardless of the timeframe being analyzed.

The matched filtering process described via Equations 1, 2, 3 makes the assumption that the noise affecting the detector is stationary [6]. Currently, the noise in LIGO detectors is described as *locally* stationary – with the exception of occasional glitches, the noise is stationary on relevant time scales, though long-period variations in the noise level occur [8].

Under these conditions, the matched filtering process should be able to correctly identify gravitational waves. However, if the noise is not stationary, matched filtering is no longer optimal; this may cause some gravitational wave signals that would otherwise be properly identified and classified to go undetected, or to be detected but with a confidence value too low to confirm their presence in the data. For these reasons, in this paper I will explore and investigate the noise in LIGO detectors to identify possible nonstationary behavior, so that either the present belief in stationary noise can be confirmed or the signal detection ability of LIGO filtering algorithms can be improved.

2 Preliminary Analysis

In order to identify nonstationary noise in the two LIGO detectors, I began by conducting a preliminary analysis of the noise to look for patterns of nonstationarity. I first created spectrograms of the data from both the Hanford and Livingston detectors, seen

in Figures 6 and 7. Spectrograms take separate raw data into slices based on time and then generate the frequency-dependent PSD for each slice of time. By doing this, spectrograms can show the noise contribution of any given frequency (on the y-axis) at any time (on the x-axis).

Spectral analysis tools and methods like spectrograms have a limit to their resolution; due to the Fourier uncertainty principle, increasing the number of slices of time decreases the number of frequencies that can be analyzed, and vice versa [9]. With this in mind, I chose to limit the frequency-domain resolution in favor of high resolution in the time-domain. As a result, in this paper I will only be able to analyze the noise level at frequencies separated by 16 Hz (e.g. 16, 32, 48 Hz, etc.). This can be seen in Figures 6 and 7 (on the next page), although the frequency axis is shown in logarithmic scale.

If the noise in the detector is stationary, the PSD should remain approximately the same over time. However, a visual inspection of the spectrograms shows that this is not the case over the long periods (ten minutes of data are used here, though actual gravitational waves signals usually only last a fraction of a second) analyzed in Figures 6 and 7.

The first can be seen at about 300 Hz, especially in Fig. 6, which has a PSD signal that seems to be oscillating over time, showing a repeated pattern of brighter and then dimmer colors several times per minute. Since I can only analyze frequencies that are multiples of 16 Hz as mentioned earlier in this section, I will, in Section 3, analyze the band of frequencies stretching from 304 Hz to 320 Hz. The second can be seen just above 500 Hz, which seems to be oscillating in PSD over time as well. In Section 4, I will investigate a bin of frequencies from 512 Hz to 528 Hz.

Finally, both the Hanford and Livingston spectrograms show long vertical lines stretching from the bottom of the plot up into frequencies on the order of hundreds of Hertz. These vertical lines indicate that the noise level at low frequencies may be frequently changing, and it may be doing so such that the noise at any of the low frequencies in the range of the vertical lines is highly correlated with the noise level of other low frequencies. I will analyze this in Section 5.

3 The 304 Hz Band

In this paper, I will use the “304 Hz band” or sometimes just “304 Hz” to refer to the range of frequencies from 304 to 320 Hz grouped into a single frequency bin due to the limitations of spectral analysis mentioned before.

I tracked the PSD value at 304 Hz over time, creating a frequency power time series (FPTS) tracking the intensity of a single frequency band over time, as seen in Figures 8 and 9 on page 5. These figures show much stronger oscillating strains in this frequency band in the Hanford detector than in the Livingston detector, which is reflected in the spectrograms.

In order to more accurately assess whether the noise at 304 Hz was oscillating in a non-stationary way, I created PSDs of the FPTSs for both Hanford and Livingston. To reduce the effect of random noise fluctuations, I sampled data from five consecutive slices of detector data spanning ten minutes each. I then averaged the resulting PSD frequency series to identify any peaks that may occur in deviation from the overall trend. These can be seen in Figures 4 and 5.

The PSDs shown in Figures 4 and 5 show some key character-

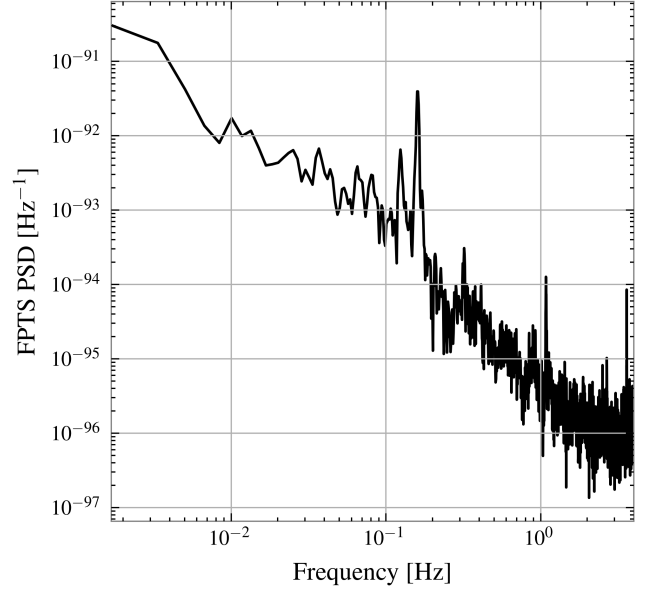


Figure 4. Average of five power spectral density plots of the 304 Hz band frequency power time series in LIGO Hanford.

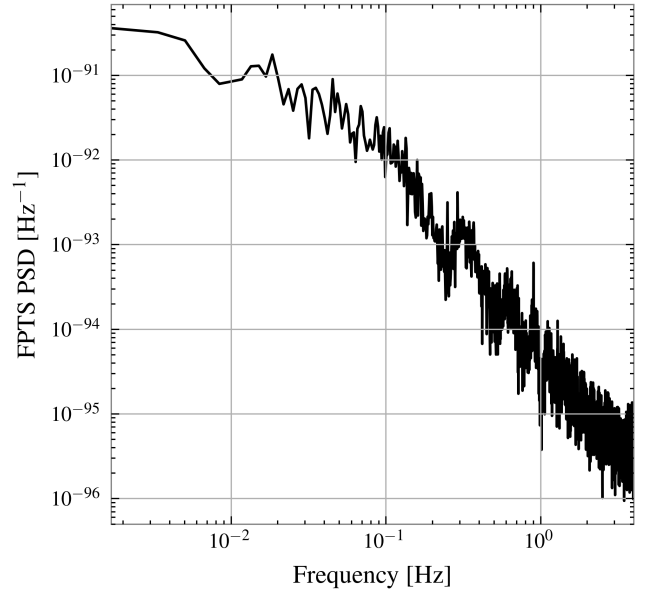


Figure 5. Average of five power spectral density plots of the 304 Hz band frequency power time series in LIGO Livingston.

istics. In both the Hanford and Livingston detectors, there is a general downward trend with an increase in frequency when the PSD is plotted on a dual logarithmic scale plot. This is expected since long-period fluctuations may more easily manifest in noise, and since the noise level is already known to drift over very long time scales.

The important characteristic traits of these PSDs is the deviation from this downward trend; in the averaged Hanford PSD, I identified three key spikes in the PSD: one at $f \approx 0.159$ Hz, a second at $f \approx 1.08$ Hz, and a third at $f \approx 3.60$ Hz. One possible source

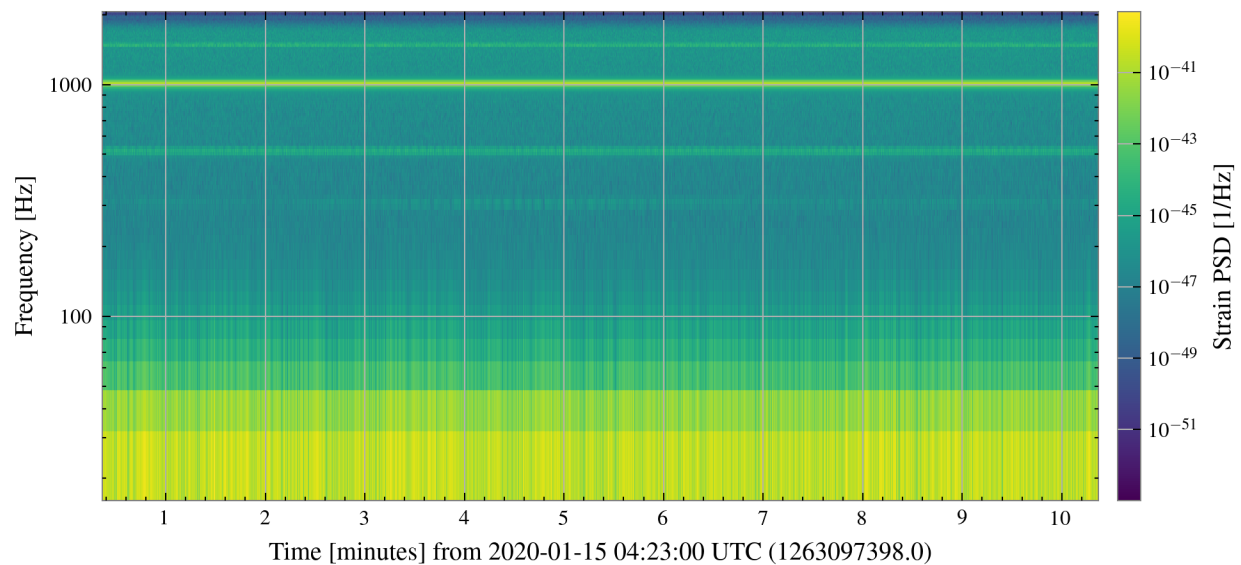


Figure 6. Ten minute spectrogram of LIGO Hanford data from January 15, 2020.

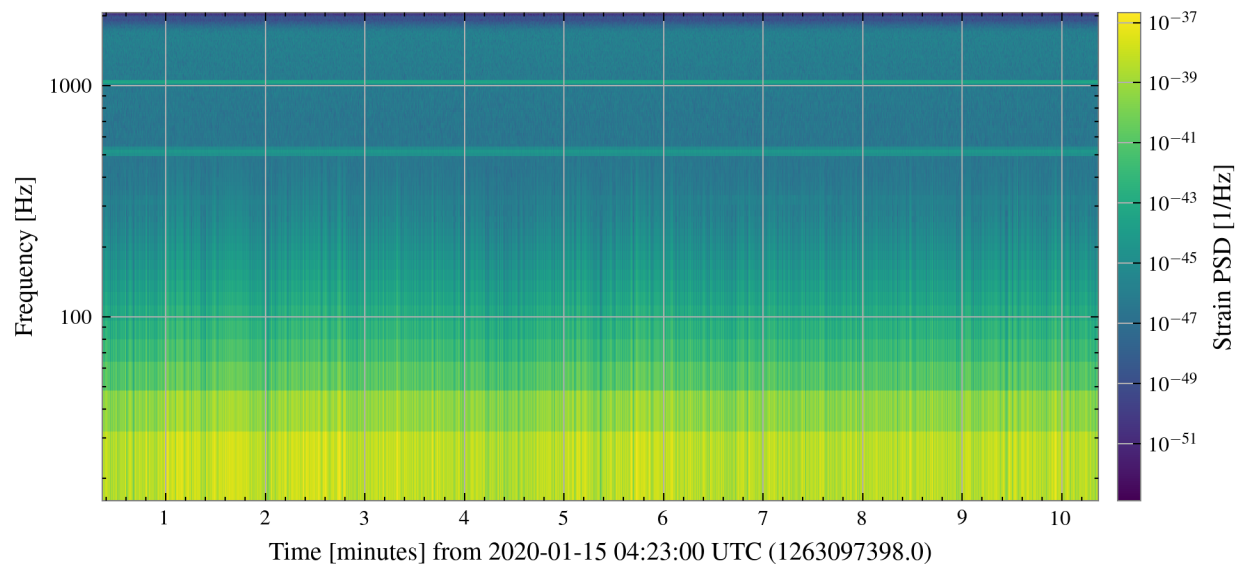


Figure 7. Ten minute spectrogram of LIGO Livingston data from January 15, 2020.

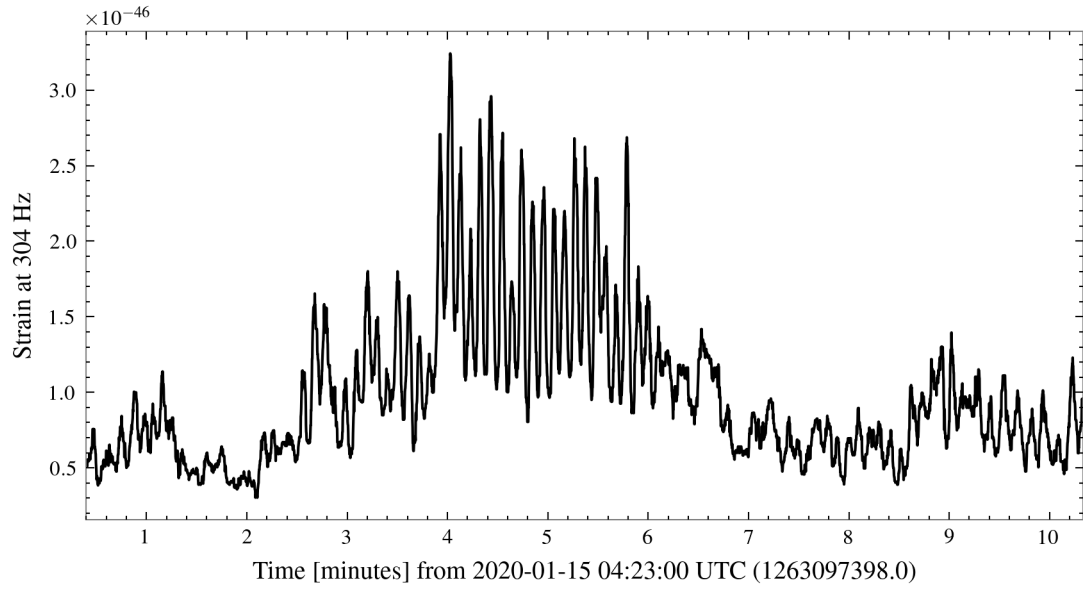


Figure 8. Ten minute 304 Hz frequency power time series of LIGO Hanford data from January 15, 2020.

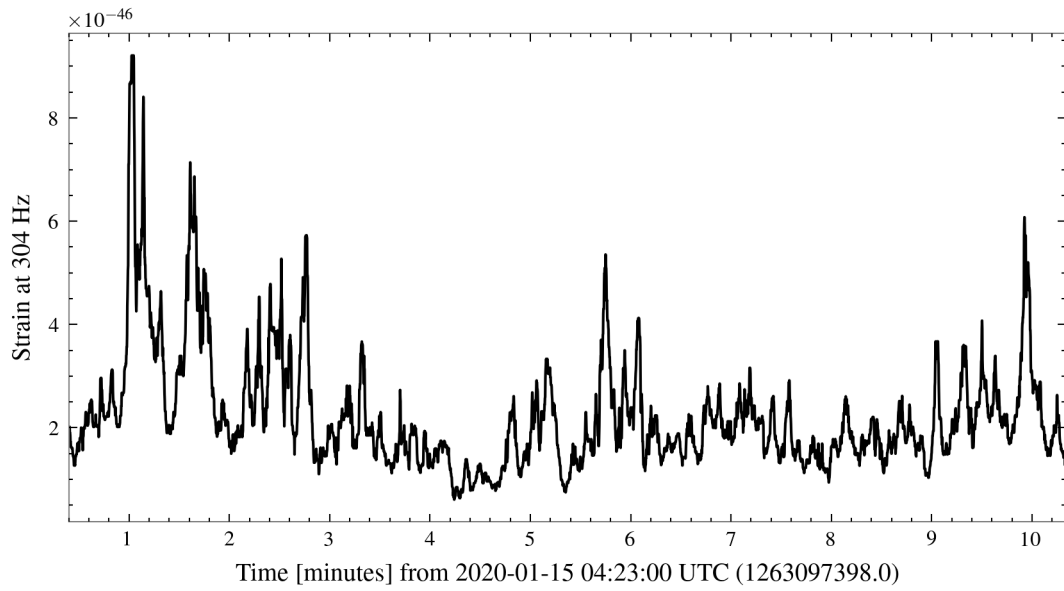


Figure 9. Ten minute 304 Hz frequency power time series of LIGO Livingston data from January 15, 2020.

of the fluctuations at 0.159 Hz is a LIGO instrument interaction with secondary microseismic noise caused by ocean waves, which can have periods around those that would cause a 0.159 frequency fluctuation [10]; however, this is highly speculative and warrants further investigation, as do the sources of both the 1.08 and 3.60 Hz phenomena in this band.

The Livingston PSDs do not show the same traits for the 304 Hz band. Since the expected distribution was unknown, I did not perform any statistical tests to identify outliers, instead using purely visual judgement. However, Figure 5 does not seem to show any peaks in the Average plot like those seen in that of Figure 4. This implies that the source of the fluctuating noise power at 304 Hz in the Hanford detector is likely limited to some quality of the instruments or location of the Hanford detector specifically, rather than something that should be expected in all LIGO or other gravitational wave detectors.

4 512 Hz Band

As mentioned in the prior section, I also investigated fluctuating noise power at 512 Hz (similar to the usage of “304 Hz”, “512 Hz” refers to a bin of frequencies from 512 to 528 Hz), using the same process used for the 304 Hz band, with results seen in Figures 10 and 11. Visually, the Hanford Average PSD is more chaotic in its general trend; there are peaks in the PSD, but they are far less distinctly identifiable. Because of this, I did not identify the frequencies of any peaks in particular until examining the Livingston data.

The 512 Hz FPTS Average PSD for Livingston data has much more defined spikes. I identified peaks at 0.087, 0.252, 0.337, 0.377, 0.549, 0.642, 0.892, 1.089, 1.667, 1.914, 2.453, 3.431, 3.466, 3.575, and 3.640 Hz. After finding the frequencies of these peaks, I reanalyzed the Hanford Average PSD and found that it did not share any of the peak frequencies shown in the Livingston Average PSD.

These findings indicate that the noise level at 512 Hz in the Livingston detector is fluctuating in a way such that these frequencies have a very strong contribution to the noise that deviates from the PSD expected at these frequencies based on the overall trend of the FPTS PSD curve. However, the causes of these peaks in PSD are unknown and must be identified in further research.

5 Correlated Noise at Low Frequencies

As seen in Figures 6 and 7, both the Hanford and Livingston detector spectrograms show vertical stripe-like features indicating that the noise levels at various low frequencies are changing at similar rates at the same times as each other. In order to determine whether this was indeed the case, I plotted the frequency power time series of 16, 32, 48, 64, 80, and 96 Hz for both the Hanford and Livingston detectors, seen in Figures 12 and 13.

These figures show that the noise levels at these low frequencies are highly correlated with each other. To analyze this effect quantitatively, I created a correlation matrix using Pearson’s correlation coefficient (see Figures 14 and 15). In this matrix, a cell at row i and column j indicates the correlation between the frequency power time series at $16i$ Hz and $16j$ Hz. For example, the cell at $i = 2$ and $j = 3$ has a value of 0.99, indicating that the Pearson’s correlation coefficient between the 32 and 48 Hz FPTSs is 0.99.

For all of these low frequencies, the correlation coefficient of the

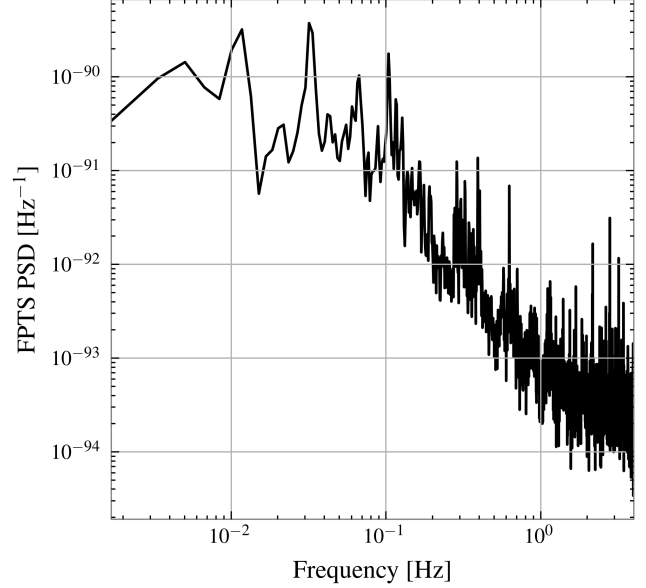


Figure 10. Average of five power spectral density plots of the 512 Hz band frequency power time series in LIGO Hanford.

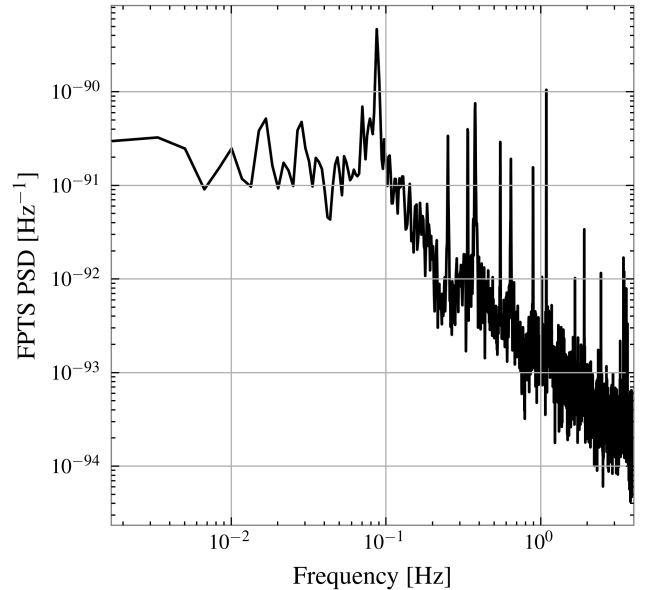


Figure 11. Average of five power spectral density plots of the 512 Hz band frequency power time series in LIGO Livingston.

FPTS with all other low frequency power time series are approximately 1, indicating a very strong relationship in their behavior. The cause of this is also unknown, however this could cause issues in the match filtering algorithms used in LIGO data analysis, though the exact way in which this would manifest is beyond the scope of this paper.

6 Conclusion

The results of my investigation show evidence of non-stationary behavior in the noise of both the Hanford and Livingston LIGO

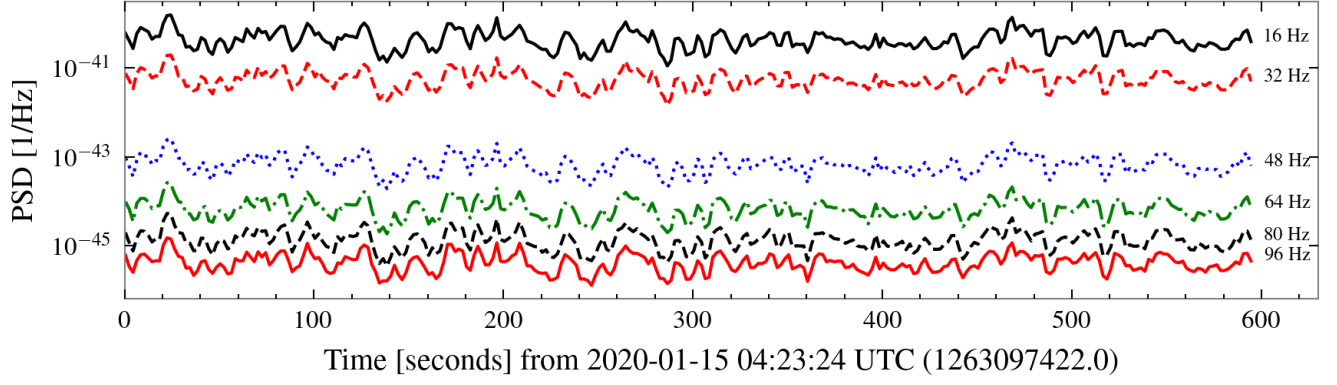


Figure 12. Frequency power time series of noise for 16, 32, 48, 64, 80, and 96 Hz in the LIGO Hanford detector.

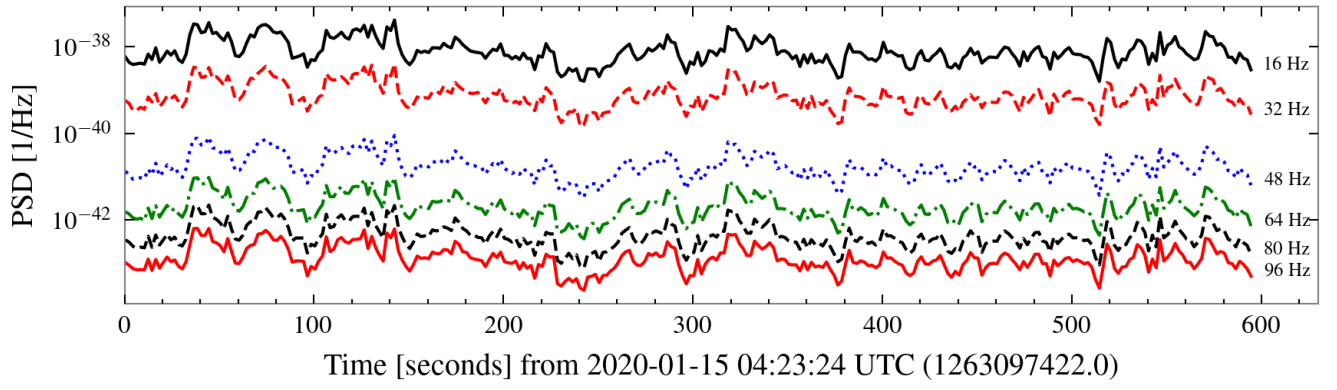


Figure 13. Frequency power time series of noise for 16, 32, 48, 64, 80, and 96 Hz in the LIGO Livingston detector.

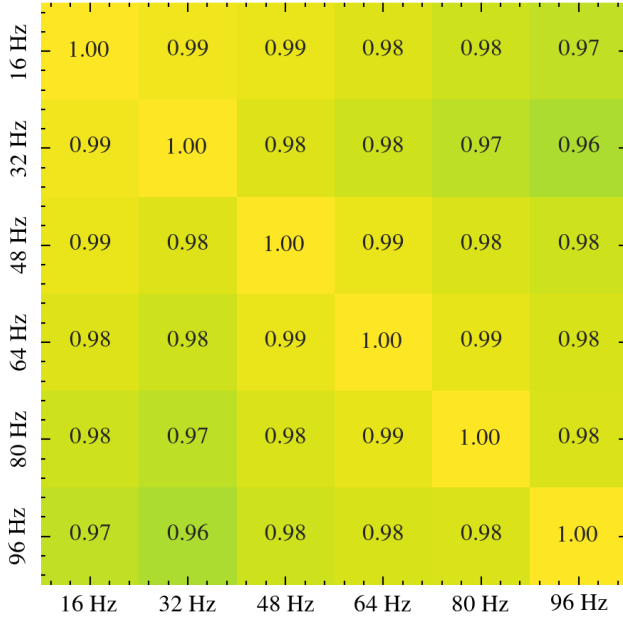


Figure 14. Correlation matrix for low frequency power time series, Hanford.

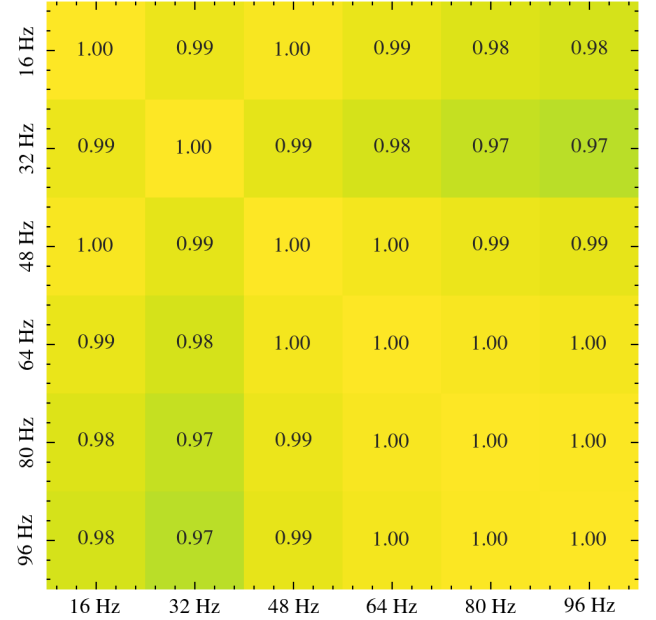


Figure 15. Correlation matrix for low frequency power time series, Livingston.

detectors. In Hanford, the 304 Hz band showed patterns of oscillation which were strong at certain frequencies, deviating from the expected noise contribution at those frequencies. The 512 Hz band showed similar patterns, which were very strong in the Livingston detector. Lastly, the noise levels at low frequencies were highly correlated with each other, with Pearson's correlation coefficients between the PSD at different frequencies below 100 Hz in both the Hanford and Livingston detectors approaching 1.0.

The sources of these non-stationary noise patterns in the LIGO detectors was not determined in this paper, and warrants further investigation in order to identify possible ways to eliminate their impact physically. Additionally, further research should investigate mathematical ways to enhance the LIGO filtering algorithms to mitigate the impact of these non-stationary behaviors.

Acknowledgements

My principle advisor for this research paper was Dr. Peter Shawhan of the Department of Physics. Additionally, I received guidance on the research process from Tristan Hightower as part of the Honors Global Challenges and Solutions program.

References

1. Wald, R. M. *General relativity* (University of Chicago press, 2010).
2. Einstein, A. & Rosen, N. On gravitational waves. *Journal of the Franklin Institute* **223**, 43–54. ISSN: 0016-0032 (1937).
3. Thorne, K. S. *Gravitational Waves* 1995. arXiv: gr-qc/9506086 [gr-qc].
4. Aasi, J. *et al.* Advanced LIGO. *Classical and Quantum Gravity* **32**, 074001. ISSN: 1361-6382 (Mar. 2015).
5. Abbott, B. P. *et al.* Observation of Gravitational Waves from a Binary Black Hole Merger. *Phys. Rev. Lett.* **116**, 061102. <https://link.aps.org/doi/10.1103/PhysRevLett.116.061102> (6 Feb. 2016).
6. Allen, B., Anderson, W. G., Brady, P. R., Brown, D. A. & Creighton, J. D. E. FINDCHIRP: An algorithm for detection of gravitational waves from inspiraling compact binaries. *Physical Review D* **85**. ISSN: 1550-2368. <http://dx.doi.org/10.1103/PhysRevD.85.122006> (June 2012).
7. Koopmans, L. H. *The spectral analysis of time series* (Elsevier, 1995).
8. Abbott, B. P. *et al.* A guide to LIGO–Virgo detector noise and extraction of transient gravitational-wave signals. *Classical and Quantum Gravity* **37**. <https://iopscience.iop.org/article/10.1088/1361-6382/ab685e> (Feb. 2020).
9. De Bruijn, N. G. *Uncertainty principles in Fourier analysis in Inequalities: proceedings of a symposium held at Wright-Patterson air force base, Ohio, August 19-27, 1965* (1967), 57–71.
10. Friedrich, A., Krüger, F. & Klinge, K. Ocean-generated microseismic noise located with the Gräfenberg array. *Journal of Seismology* **2**, 47–64 (1998).